ELSEVIER

Fuel Processing Technology 64 (2000) 73–105

FUEL PROCESSING TECHNOLOGY

www.elsevier.com/locate/fuproc

Design and scale-up of the Fischer–Tropsch bubble column slurry reactor

R. Krishna [a,*], S.T. Sie [b]

[a] *Department of Chemical Engineering, University of Amsterdam, Nieuwe Achtergracht 166, 1018 WV Amsterdam, Netherlands*

[b] *Faculty of Chemical Technology and Materials Science, Delft University of Technology, Julianalaan 136, 2628 BL Delft, Netherlands*

Received 12 July 1999; received in revised form 2 November 1999; accepted 10 December 1999

Abstract

The Fischer–Tropsch (FT) synthesis on a large scale is of interest, as a means of conversion of remote natural gas to high-quality products, particularly, liquid transportation fuels. Recent developments have resulted in reactors of advanced design having production capacities of 2500 bbl/day or higher, which is more than two orders of magnitude higher than the productivity of classical reactors operated before or during World War II. Some fundamental aspects of these reactors, which belong to the classes of gas–solid fluidised beds, multi-tubular trickle-beds, and slurry bubble columns, are discussed to aid the selection and design of reactors for a specific application.

Special attention is given to scaling up of slurry bubble columns. Published experimental work is carefully analysed, and procedures are recommended for the estimation of the necessary design and scale-up parameters. Model calculations of a commercial FT reactor are presented in order to underline various important design and operating issues.

Keywords: Fischer–Tropsch synthesis; Reactors; Fluidised bed; Multi-tubular trickle bed; Slurry bubble columns; Scaling-up

1. Introduction

The Fischer–Tropsch (FT) reaction that was discovered in Germany nearly three quarters of a century ago, has recently become a subject of renewed interest, particularly

* Corresponding author. Fax: +31-20-5255604.
E-mail address: krishna@chemeng.chem.uva.nl (R. Krishna).

0378-3820/00/$ - see front matter
PII: S0378-3820(99)00128-9

in the context of the conversion of remote natural gas to liquid transportation fuels. The main incentives for this conversion are the increased availability of natural gas in remote locations, for which no nearby markets exist, and the growing demand for middle distillate transportation fuels (gasoil and kerosine), especially in the Pacific and Asian regions. Natural gas can be converted to carbon monoxide and hydrogen (synthesis gas) via the existing or newly developed processes, such as steam reforming, carbon dioxide reforming, partial oxidation, and catalytic partial oxidation, followed by the FT synthesis reaction

$$CO + 2H_2 \rightarrow ``{-}CH_2{-}'' + H_2O + 170\,kJ$$

in which ''$-CH_2-$'' represents a product consisting mainly of paraffinic hydrocarbons of variable chain length. In most cases, the chain length distribution of the product follows an Anderson–Schulz–Flory distribution function characterised by a chain growth probability factor α_{ASF}.

For economic and logistic reasons, such energy conversions are best carried out in large scale projects and the capability of upscaling is therefore an important consideration in the selection of reactors for synthesis gas generation, as well as in FT synthesis. Another important issue in FT synthesis is the strong exothermicity: e.g., compared to the processes applied in the oil industry, the heat released per unit weight of feed or product is an order of magnitude higher, and corresponds with a theoretical adiabatic temperature rise of about 1600 K at complete conversion. Unless the product is so light that it is completely vaporised under reaction conditions, the reaction takes place in a three-phase system: gas (carbon monoxide, hydrogen, steam, and gaseous hydrocarbon products), liquid product, and solid catalyst. The amounts of syngas and product molecules that have to be transferred between the phases are quite large: i.e., an order of magnitude larger than the amount of hydrogen molecules to be transferred in hydroprocessing of oils. Therefore, great demands are placed on the effectiveness of interfacial mass transfer in FT synthesis.

The present paper discusses the selection of FT reactors against this background and compares the limitations, advantages, and disadvantages of alternative reactor types based on some fundamental principles.

The bubble column slurry reactor will be singled out for special attention and the design and scale-up parameters for this reactor type discussed on the basis of a careful analysis of the published literature.

2. Developments in reactors for FT synthesis

Commercial scale FT reactors have been installed and operated before and during World War II in a number of plants, mostly in Germany. In addition to these commercially applied reactors (which are very small by current standards), several other reactor types have been proposed and developed to varying degrees of commercial readiness in the period before and during World War II. These early reactor types are discussed below.

(A) Fixed-bed reactor with internal cooling operated at high conversion in a once-through mode. The catalyst was packed in a rectangular box and water-cooled tubes fitted with cooling plates at short distances were installed in the bed to remove the reaction heat. This type of reactor was applied in the atmospheric synthesis process (''Normaldruck Synthese'') (see Fig. 1a).

(B) Multi-tubular reactor with sets of double concentric tubes, in which the catalyst occupied the annular space, surrounded by boiling water. This type of reactor was applied with gas at medium pressure in a once-through mode (''Mitteldruck Synthese''). The configuration is the same as shown in Fig. 1a.

(C) Adiabatic fixed-bed reactor with a single bed, large recycle of hot gas, which was cooled externally (''IG-Farben/Michael Verfahren'') (see Fig. 1b).

(D) Fixed-bed reactor with multiple adiabatic beds, inter-bed quenching with cold feed gas, recycle of hot gas and external cooling (''Lurgi Stufenoven'') (see Fig. 1c).

(E) Adiabatic fixed-bed reactor with a large recycle of heavy condensate passing in upflow through the bed. The liquid recycle stream was cooled externally (''BASF/Duftschmid Verfahren'') (see Fig. 1d).

(F) Slurry reactor with entrained solid catalyst, large recycle of hot oil and external cooling (''BASF Schaumverfahren'') (see Fig. 1e).

More details on these reactors can be found in the literature on the FT process, e.g., in reviews of Kölbel [1] and Roelen et al. [2]. The above reactors are mainly of historical interest since they offer limited scope for the large-scale conversion of natural gas to liquid hydrocarbons. The commercially applied reactors mentioned under (A) and (B) have very small production capacities by current standards, viz., of the order of 0.1 ton/h or 15 bbl/day. At the low gas velocities associated with once-through operation at relatively low pressures and temperatures, heat transfer rates from the bed to the cooling surface are so low that a very large cooling area is required, which is a strong limiting factor in further upscaling.

The other reactors with external cooling need very large recycle streams to take up and transport the generated heat out of the reactor. This gives rise to high pressure drops and very high energy consumption for gas or liquid circulation, if the reactors were to be applied in FT synthesis on a very large scale. These reactor types will therefore not be considered further in the present context of remote natural gas conversion.

Developments in the period shortly after World War II (in some cases, based on concepts generated somewhat earlier) led to reactors with increased potential for large-scale production of synthetic fuels. The main ones are discussed below.

(A) A multi-tubular fixed-bed reactor operated with gas recycle at moderate per pass conversion (see Fig. 1f), instead of once-through operation aiming at maximum conversion as in the earlier mentioned ''Mitteldruck Synthese''. This reactor, applied in the ''Arge Hochlast Synthese'' developed by Lurgi and Ruhrchemie, has a production capacity of about 50 tons/day (about 400 bbl/day). This substantially increased production rate, as compared with the previous commercial fixed-bed reactors (by a factor of about 25), is the result of higher temperatures and pressures; a more uniform reaction rate profile over the reactor length and improved heat removal as a result of the higher gas velocities [3]. A commercial plant based on the Arge process was installed by the South African Coal, Oil and Gas (Sasol) at Sasolburg in South Africa [4,5]. The

effect of recycling will be discussed in more detail in a later section dealing with fundamental aspects of multi-tubular fixed-bed FT reactors.

(B) Slurry reactor, in which synthesis gas is contacted in a bubble column with slurry of fine catalyst suspended in liquid. In the process developed by Rheinpreussen and Koppers in the early 1950s [6–8], reaction heat is removed internally by cooling pipes immersed in the slurry (see Fig. 1g). The development studies culminated in the operation of a semi-commercial reactor of 10 m^3 effective volume (about 7.5 m high and of 1.3 m diameter) having a capacity of 10 tons/day (about 80 bbl/day). For this reactor, a high (about 90%) conversion of carbon monoxide has been reported when operated in a gas once-through mode at a superficial gas velocity of about 0.1 m/s [8].

(C) Three-phase fluidised bed (ebulliated bed, also called ebbulating bed) reactor, in which a packing of larger catalyst particles (e.g., 8–16 mesh) is expanded by cocurrent upflow of oil and gas. The process studied by the US Bureau of Mines features circulation of oil for attaining sufficiently high liquid velocities and has therefore been referred to as the oil circulation process (see Fig. 1h). Process development studies were carried out in a 3-gal/day pilot reactor of 3.2 m length and 7.5 cm diameter, and also in a 1-bbl/day reactor of 20 cm diameter with a bed height of 2.4 m [9–11]. The process has not been commercialised.

(D) Fluidised-bed reactor operated in the bubbling regime, as used in the Hydrocol process for producing gasoline from natural gas [12] (see Fig. 1i). Reaction heat is removed by vertical bundles of cooling tubes submersed in the bed. A commercial plant has been erected in Brownsville, TX by Carthage Hydrocol, featuring a reactor of 18 m height and 4 m diameter with a nominal capacity of 180,000 tons/year. Due to technical, as well as economic problems, the plant has been in operation for a short period only before being shut down in 1956.

(E) Circulating fluid-bed system, in which fine catalyst (between 40 and 150 μm diameter) is entrained by a high velocity (1–2 m/s) gas stream through a riser reactor (see Fig. 1j). Catalyst separated from the effluent by cyclones is returned to the reactor inlet. Two cooling zones in the riser remove reaction heat. The process originally developed by the Kellogg as the Synthol process [13] has been commercialised and further improved by Sasol. In the first commercial plant that began operation in 1955 at Sasolburg in South Africa, Synthol reactors of 2.3 m diameter and a total height of

Fig. 1. (a) Fixed-bed reactor configuration; gas once-through (Classical Fischer–Tropsch: ''Normal Druck Synthese'' and ''Mittel Druck Synthese''). (b) Fixed-bed reactor configuration with large recycle of hot gas (single adiabatic bed) (I.G. Farben/Michael Verfahren). (c) Fixed-bed reactor with large recycle of hot gas (multiple beds) (Lurgi Stufenofen). (d) Fixed-bed reactor with large recycle of heavy condensate (BASF/Duftschmid Verfahren). (e) Slurry reactor (entrained solids) with large recycle of hot oil (BASF Schaumverfahren). (f) Fixed-bed reactor with partial conversion and recycle of unconverted gas (Arge Hochlast Synthese). (g) Slurry reactor with in-situ cooling (Rheinpreussen–Koppers Synthese). (h) Expanded bed reactor with large recycle of hot oil and moderate recycle of gas (US Bureau of Mines oil circulation process). (i) Stationary fluid-bed process with moderate recycle of unconverted gas (Hydrocol process). (j) Riser reactor with catalyst and gas recycle (Synthol process). (k) Schematic of the SMDS process which involves heavy paraffin synthesis, followed by the hydrocracking of the paraffins to produce products predominantly in the diesel range. A multi-tubular trickle-bed reactor is used in the Fischer–Tropsch synthesis step. For process description see Sie [15].

46 m, with a capacity of 1500 bbl/day were installed. Considerably scaled-up reactors with a capacity of 6500 bbl/day were later installed in Sasol II and III located in Secunda in the Witwatersrand area and began operation in 1980 and 1982, respectively.

In the last 20 years, revived interest in the FT process in the context of conversion of remote natural gas gave rise to several developments of more advanced reactors with

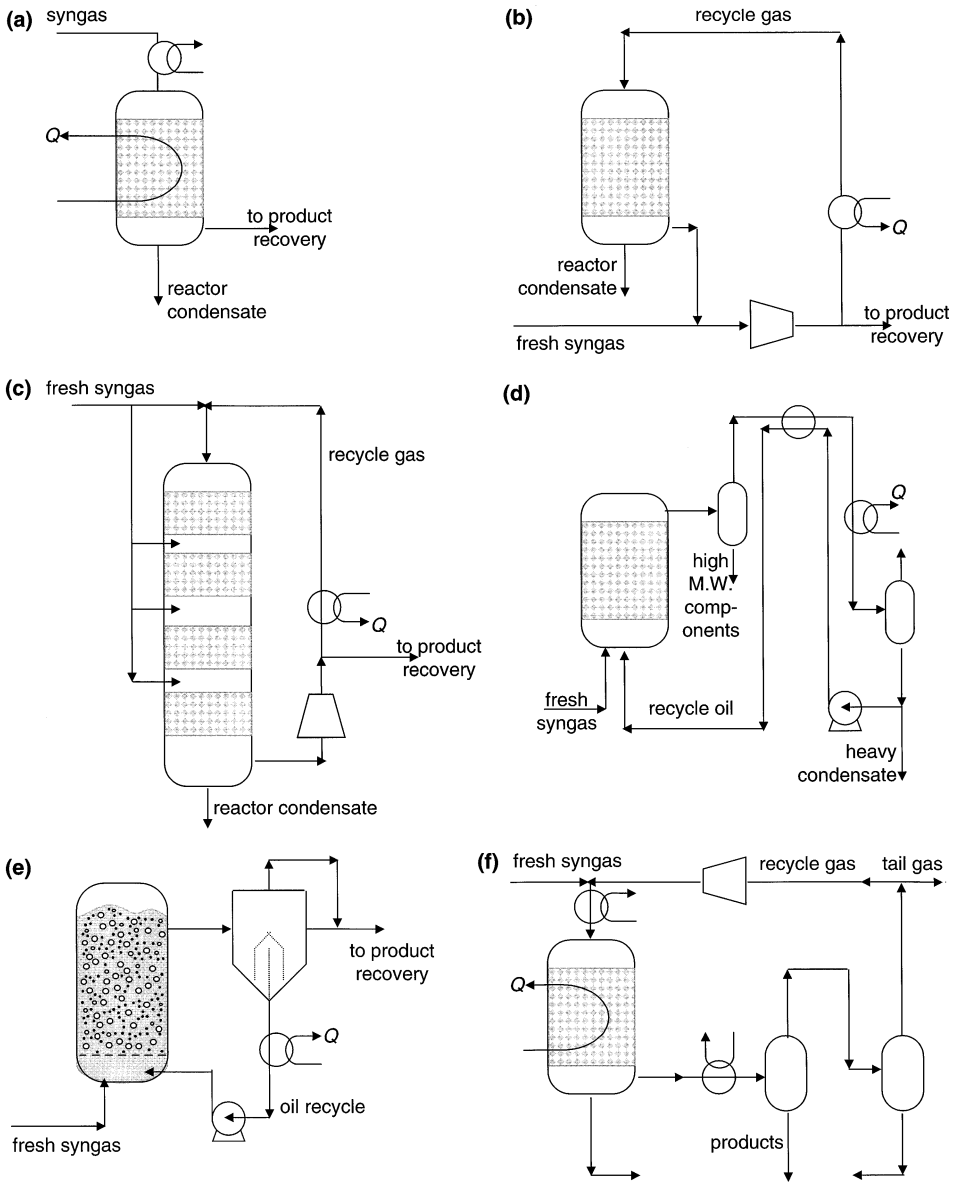

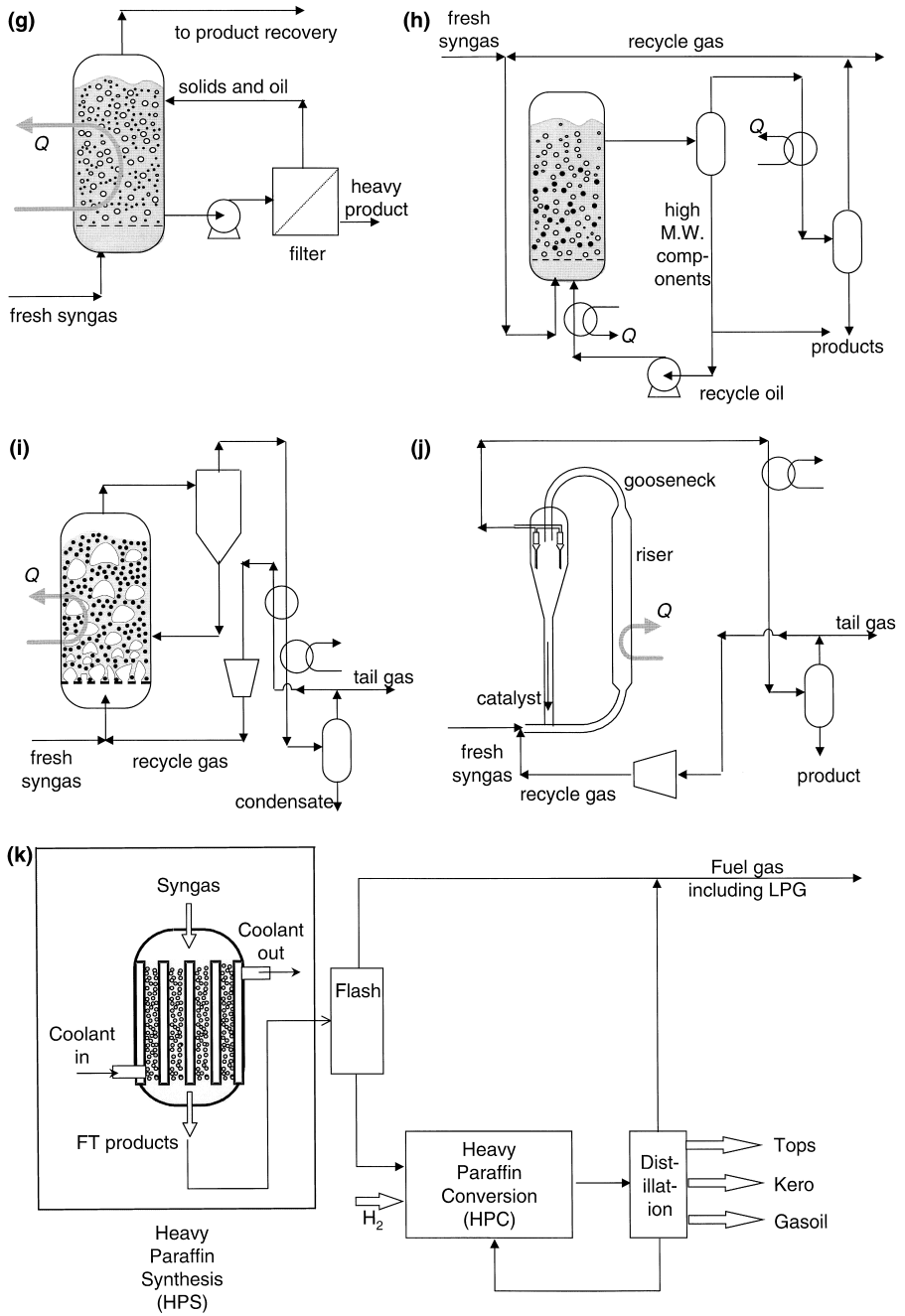

Fig. 1 (*continued*).

(potentially) large capacities that have been commercialised or can be considered to be ready for commercialisation. These reactors are mentioned below.

(A) A bubbling fluidised-bed version of the Synthol process has been developed by Sasol and the first commercial scale reactor has started operation in Sasolburg in 1989 [14]. This reactor, which like the previously discussed Hydrocol reactor (see Fig. 1i), operates in the bubbling regime and is internally cooled by cooling tubes, has considerable advantages over the original circulating fluid-bed version of the Synthol process. Claimed advantages include a more compact reactor for the same capacity (in particular reduced height), less energy required for gas circulation, less catalyst attrition, and easier operation and maintenance, resulting in substantial reductions in capital and operating cost.

The size advantage of the bubbling fluidised version of the Synthol process stands to reason, because the FT reaction is a relatively slow one, even at the high temperatures applied in the Synthol process. From a theoretical reactor engineering point of view, a riser is therefore not the optimal type of reactor due to the low catalyst density in the reactor space.

As mentioned before, the FT reaction is a highly exothermic one and therefore, gas–solid fluidised-beds, with their excellent heat transfer and temperature equalisation characteristics are very attractive. The use of small catalyst particles, e.g., of about 100 μm diameter, ensures freedom from pore diffusion limitations. However, a serious issue is the possibility that heavy product deposits on the catalyst, causing particles to agglomerate, and thus, hampering fluidisation. To avoid this problem, commercial gas–solid fluidised FT processes operate at relatively high temperature and moderate pressure, producing a relatively light product of low α_{ASF} value (< 0.71). The condition that α_{ASF} must be less than 0.71 rules out the possibility of applying gas–solid fluidised-beds for FT processes that produce much heavier products than gasoline. Even when low operating pressures and relatively high temperatures are adopted, the heavier tail of a high α_{ASF} product will inevitably condense on the catalyst particles. Therefore, only reactors, in which a liquid phase is present besides the gas and solid catalyst phases, are eligible for producing such products. Such type of reactors is discussed in (B) and (C) below.

(B) Multi-tubular reactor as applied in the Shell Middle Distillate Synthesis (SMDS) process for the conversion of synthesis gas in a heavy, waxy FT product [15] (see Fig. 1k). Reactors of this type have been installed in the first SMDS plant at Bintulu, Malaysia for the production of some 470,000 tons/year of synthetic hydrocarbons from natural gas starting from 1993. With a specially developed catalyst and a specific reactor design, a capacity of about 3000 bbl/day per reactor is attained, which is an order of magnitude larger than the capacity of the multi-tubular reactor of the Arge design.

Because of pressure drop constraints, catalysts in fixed-bed processes generally have diameters larger than about 1 mm. For particles of this size, intraparticle diffusion can be a limiting factor for the overall reaction rate [16]. Studies with porous iron and cobalt catalysts under conditions, which ruled out external mass transfer effects, have confirmed the occurrence of diffusion limitation and made it plausible that diffusion of reactants and product molecules through liquid-filled pores is the determining factor in intraparticle transport of mass. For FT catalysts with the usual chemical activities, this

means that intraparticle diffusion starts to play a role for particle diameters greater than about 0.5 mm. Intraparticle diffusion is therefore an important factor to be taken into account in choosing catalyst particle size and shape for a fixed-bed FT process, in addition to pressure drop and heat transfer considerations.

A multi-tubular reactor, in which the catalyst-filled tubes are surrounded by a cooling medium, such as boiling water, the reactor is, at least conceptually, an isothermal reactor and the heat of the reaction should therefore be removed by radial transport. The relatively poor heat conductivity and heat transfer to the tube wall as compared with fluidised-beds easily give rise to radial temperature profiles. In an extreme case, the reactor can become unstable and temperature may run away. However, even in the stable operating region, unduly large temperature peaks in the bed are to be avoided as they may give rise to an undesired reduction of selectivity or accelerated catalyst activity decline.

Aside from the choice of tube diameter, which is governed by constructional and cost considerations, catalyst particle size and gas velocity determine the effectiveness of radial heat transport and the homogeneity of temperature in the bed. The radial heat conductivity, as well as the transfer coefficient, becomes higher with increasing Reynolds number. The heat removal becomes more effective with larger particles and at higher velocities. Limiting factors to an increase of particle size and velocity are the effectiveness of the catalyst and pressure drop.

Since axial mixing and axial heat transport in the long tubes of a multi-tubular reactor are relatively low, profound axial concentrations and temperature profiles can be present, particularly when one targets for a high conversion in a once-through operation as in the classical fixed-bed processes [1]. Strong radial temperature profile in the region near the inlet, since in this region, the reaction rates are high because of the high partial pressure of the reactants. Further down the reactor tubes, rates are much lower as the reactants are being depleted, and therefore, radial temperatures are more even. Since the tube and catalyst dimensions have to be designed to cope with the strongest temperature peaks, it follows that the larger part of the tube is overdesigned, or in other words, does not fully utilise the potential within the existing constraints.

More uniform axial profiles of reactant concentration, local reaction rates and temperature in the axis of the tube are obtained when the conversion is restricted to, for instance, 20–30% per pass instead of more than 70%. Because of the recycling of the unconverted gas, linear velocities are increased, and this has a beneficial effect on the effectiveness of heat removal (see above). The Arge process mentioned earlier, derives its advantages over the classical multi-tubular fixed-bed process from the application of gas recycle in combination with higher temperature and pressures: an enhancement of reactor capacity by a factor of 25, a reduction of the cooling area by a factor 12, and a lowering of the amount of catalyst and steel by a factor of about 7 [3].

An improvement of radial heat conductivity and heat transfer to the wall cannot only be obtained by increasing the linear gas velocity in a gas–solid fixed-bed multi-tubular reactor, but also by operating in the presence of liquid [17]. In the case of a FT reaction producing a relatively heavy product, the reactant stream is initially a gas that changes to a gas/liquid mixture in the flow direction as condensable product is being produced. In this situation, the effectiveness of heat removal will be lowest in the inlet region, where

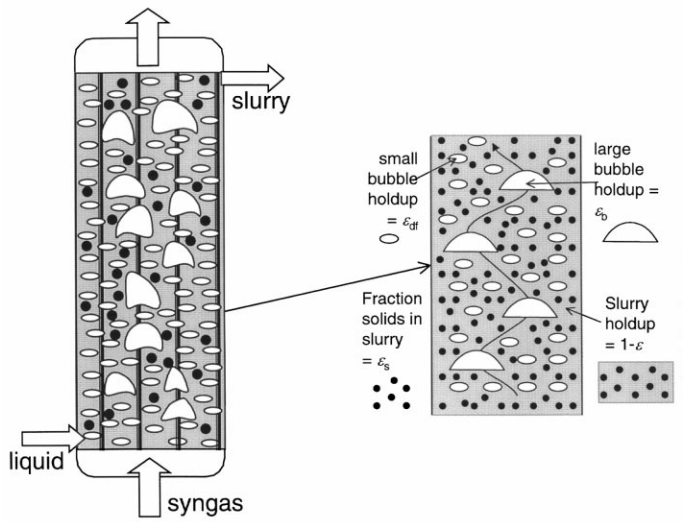

Fig. 2. The bubble column slurry reactor configuration with internal cooling. On the right is a simplified description of the various phases, which is used in this paper.

the reaction rates are highest. By adding liquid, one can ensure that the whole tube, including the most critical part, operates in a trickle-flow mode, instead of just the bottom part.

(C) An internally cooled bubble column slurry reactor shown schematically in Fig. 2. Sasol has developed an internally cooled slurry reactor as an alternative to the multi-tubular fixed-bed reactors of the Arge process [18,19]. A commercial reactor of 5 m diameter and 22 m height designed for a capacity of about 2500 bbl/day was commissioned in 1993. The Sasol Slurry Bed Reactor (SSBR) technology is now considered by Sasol to be commercially proven and the design of a 10,000-bbl/day plant is being considered. A parallel development of the bubble column slurry reactor technology is due to Exxon as part of their Advanced Gas Conversion technology. A demonstration reactor with a diameter of 1.2 m in a 21-m-high structure has been erected in 1990 at Exxon's R&D laboratory at Baton Rouge, LA [20,21]. Based on operating experience with this unit that achieved a production rate approaching 200 bbl/day, Exxon feels confident that a commercial-scale unit can be designed and constructed.

3. Multi-tubular fixed-bed reactor vs. bubble column slurry reactor

For the reasons discussed in Section 2, the viable reactor choices for a commercial process aimed at the production of relatively heavy hydrocarbon products are the multi-tubular fixed-bed operating in the trickle-flow regime (see Fig. 1k) and the bubble column slurry reactor (Fig. 2). These two reactor types can be built with substantially

higher capacities (2500 bbl/day or higher) than the reactors developed before, during, and shortly after World War II. The maximum feasible capacity is not fixed; however, other factors, besides the fundamental limitations discussed so far, can play a role. Aside from the mechanical construction aspects, the weight of the reactor can be a limiting factor if the reactor has to be transported and erected in remote areas with poorly developed infrastructure. For offshore installation on fixed and floating platforms, other limiting criteria, such as the floor space needed and the maximum height may apply. Interest in offshore production of synthetic fuels appears to be mounting, as indicated by recently announced alliance between the Norwegian Oil Company Statoil and Sasol for developing this option (See information and press releases of Sasol, Cavan Hill, South Africa, posted on their internet web site in Ref. [22]).

For the specific case of the conversion of syngas into a relatively heavy FT product, De Swart et al. [23] have compared the multi-tubular trickle-bed reactor with slurry reactors operating in either the homogeneous or the heterogeneous regime. With a maximum weight of 900 tons/reactor as limiting criterion, the number of reactors needed for a plant capacity of 5000 tons/day (approximately 40,000 bbl/day) were found to be 10 for the multi-tubular trickle bed, 17 for the slurry reactor operating in the homogeneous regime, and four for the bubble column slurry reactor operating in the heterogeneous flow regime.

While the maximum achievable capacity in FT reactors is undoubtedly a very important factor in the economy of large-scale natural gas conversion, it is not the only one that governs reactor choice. Reactor costs may differ for different reactors of equal capacity, depending upon the complexity of construction. In addition, in this regard, the slurry bubble column may compare favourably with the multi-tubular fixed-bed.

4. Bubble column slurry reactor design parameters

In view of the foregoing arguments, we believe that the bubble column slurry reactor is the best choice of reactor type for large-scale plants with capacities of the order of 40,000 bbl/day. Successful commercialisation of this technology is crucially dependent on the proper understanding of the scaling-up principles of bubble columns for the above mentioned conditions fall outside the purview of most published theory and correlations in standard text books [24,25]. We discuss the design and scale-up aspects of this reactor type in detail below, relying heavily on the experimental research carried out during the last decade or so at the University of Amsterdam [26–44].

4.1. Hydrodynamic regimes and influence of increased particles concentration

When a column filled with a liquid is sparged with gas, the bed of liquid begins to expand as soon as gas is introduced. As the gas velocity is increased, the bed height increases almost linearly with the superficial gas velocity U provided the value of U stays below a certain value U_{trans}. This regime of operation of a bubble column is called the *homogeneous bubbly flow regime*. The bubble size distribution is narrow, and a roughly uniform bubble size, generally in the range 1–7 mm, is found. When the

superficial gas velocity U reaches the value U_{trans}, coalescence of the bubbles takes place to produce the first fast-rising ''large'' bubble. The appearance of the first large bubble changes the hydrodynamic picture dramatically. The hydrodynamic picture in a gas–liquid system for velocities exceeding U_{trans} is commonly referred to as the *heterogeneous or churn–turbulent flow regime* [26,28,29,31]. In the heterogeneous regime, small bubbles combine in clusters to form large bubbles in the size ranging from 20 to 70 mm [31]. These large bubbles travel up through the column at high velocities (in the 1–2 m/s range), in a more or less plug flow manner [26,32,36]. These large bubbles have the effect of churning up the liquid phase [30]. The large bubbles are mainly responsible for the throughput of gas at high velocities [26,30]. Small bubbles, which co-exist with large bubbles in the churn–turbulent regime, are ''entrained'' in the liquid phase, and as a good approximation, have the same backmixing characteristics of the liquid phase [30]. The two regimes are portrayed in Fig. 3, which also shows in a qualitative way, the variation of the gas hold-up ε as a function of the superficial gas velocity U. When the gas distribution is very good, the regime transition point, U_{trans}, is often characterised by a sharp maximum in the gas hold-up [28]. The same picture, as shown in Fig. 3, holds for a bubble column slurry reactor when fine catalyst particles (typically smaller than 50 μm) are used [29,33]. The fine catalyst particles are intimately mixed with the liquid, and the slurry phase can be considered to be pseudo-homogeneous. The assumption of a pseudo-homogeneous slurry phase, where no catalyst settling takes place, is a good one for operation of large diameter columns (say larger than 0.5 m) at high superficial gas velocities ($U > 0.2$ m/s).

When the concentration of solid particles (catalyst) in the liquid increases, the total gas hold-up, ε, is reduced. The data for paraffin oil slurries to which silica particles

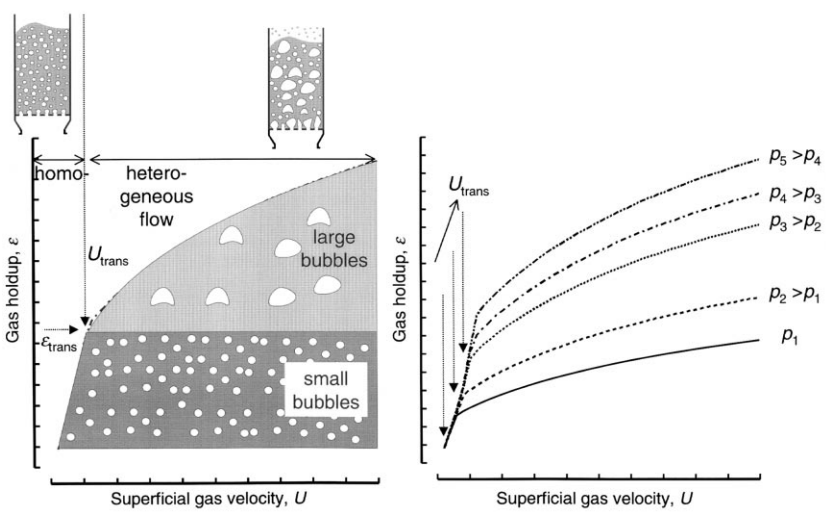

Fig. 3. Homogeneous and churn–turbulent regimes in a gas–liquid bubble column [28,30]. The figure on the right shows that increasing the system pressure delays the regime transition point.

(mean particle size of 38 μm) have been added illustrates this effect [33] (see Fig. 4). Note the sharp maximum in the total gas hold-up near the regime transition point for slurry concentrations smaller than 10%.

The dynamic gas disengagement experiment [26,32] allows us to determine the hold-up of gas in the ''small'' and ''large'' bubbles. In this experiment, the gas supply to a column operating under steady-state is switched off instantaneously at time $t = 0$, and the dispersion height is monitored as a function of time by means of a pressure sensor located in the column at a given height. Typical dynamic gas disengagement profiles for air — paraffin oil and air — 36 vol.% paraffin oil slurry in the 0.38-m column for the churn–turbulent flow regime of operation are shown in Fig. 5. After the shut-off of the gas supply, the hold-up decreases due to the escape of fast rising ''large'' bubbles (''dilute'' phase). When the ''large'' bubbles have escaped, the ''small'' bubbles leave the column. The voidage of gas in the ''dense'' phase, ε_{df}, is determined as indicated in Fig. 5. The gas hold-up of the ''large'' bubbles, i.e., ''dilute'' phase is obtained from $\varepsilon_b = (\varepsilon - \varepsilon_{df})/(1 - \varepsilon_{df})$. The terminology of ''dilute'' and ''dense'' phases is based on the ''two-phase'' model adopted earlier to describe the hydrodynamics of bubble columns in the churn–turbulent flow regime experiments [26,32]; this model is adapted for slurry bubble columns in Fig. 6. The slope of the second, slowly disengaging portion of the bed-collapse curves in Fig. 5 yields the superficial gas velocity through the dense phase, U_{df}. The superficial gas velocity through the ''dense'' phase, U_{df}, can be taken to be equal to U_{trans}.

It is clear from the dynamic gas disengagement experiment shown in Fig. 5 that the decrease in the total gas hold-up in more concentrated slurries is primarily caused of the

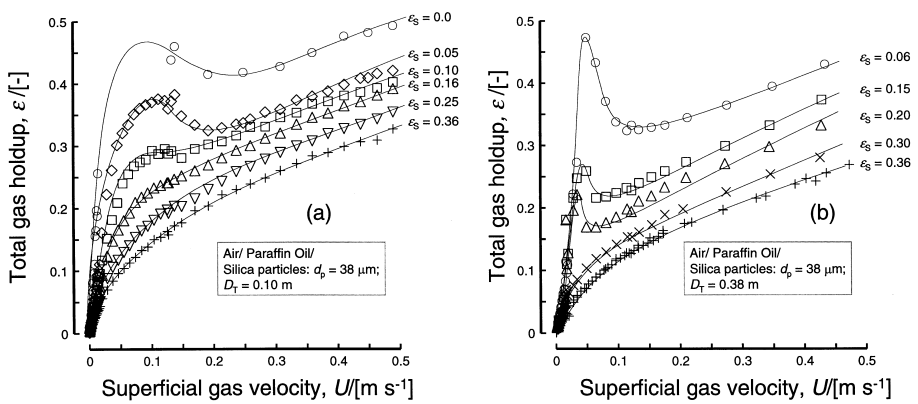

Fig. 4. Influence of increased particles concentration on the total gas hold-up in columns of (a) 0.1 m and (b) 0.38 m diameter. The experimental data is from Krishna et al. [33]. Air was used as the gas phase in all experiments. The liquid phase was paraffin oil (density, $\rho_L = 790$ kg m^{-3}; viscosity, $\mu_L = 0.0029$ Pa s; surface tension, $\sigma = 0.028$ N/m) to which solid particles in varying concentrations were added. The solid phase used consisted of porous silica particles (skeleton density = 2100 kg m^{-3}; pore volume = 1.05 ml g^{-1}; particle size distribution, d_p: 10% < 27 μm; 50% < 38 μm; 90% < 47 μm). The solids concentration ε_s, is expressed as the volume fraction of solids in gas free slurry. The pore volume of the particles (liquid-filled during operation) is counted as a part of the solid phase.

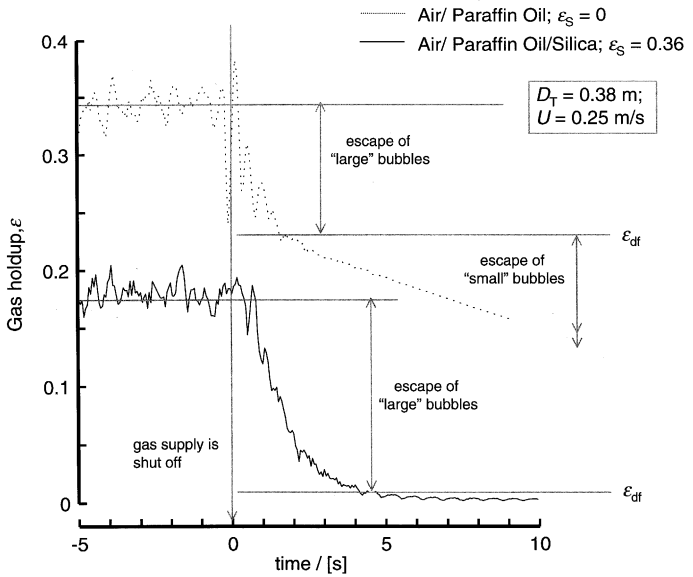

Fig. 5. Dynamic gas disengagement experiments for air/paraffin oil and air/36 vol.% paraffin oil slurry in the 0.38-m-diameter column. The experimental data is from Krishna et al. [33]. The system properties are as given in the legend to Fig. 4.

decrease in the hold-up of the small bubbles. This decrease in small bubble hold-up due to enhanced coalescence resulted in the presence of the small particles. The destruction

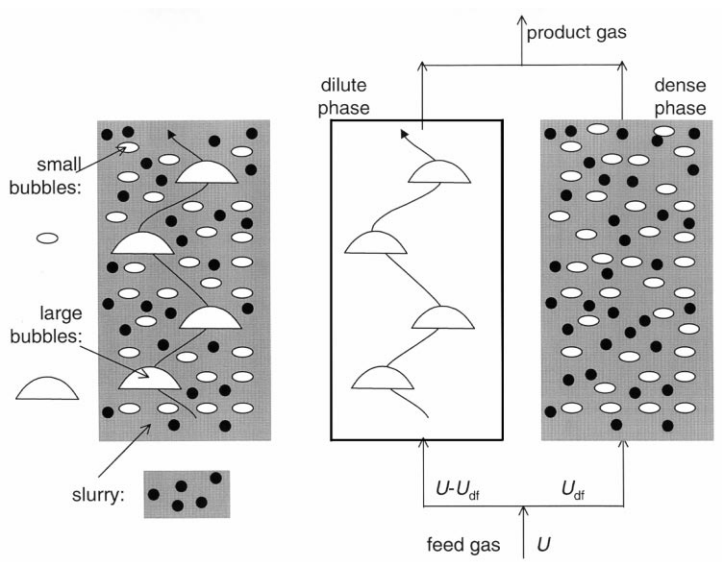

Fig. 6. Generalized two-phase model applied to a bubble column slurry reactor operating in the churn–turbulent regime [28–30].

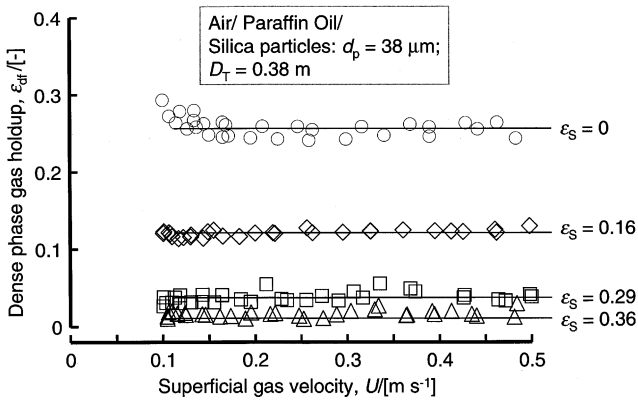

Fig. 7. Influence of increased solids concentration on the dense phase gas hold-up for air/paraffin oil slurries in a 0.38-m-diameter column. The experimental data is from Krishna et al. [33]. The system properties are as given in the legend of Fig. 4.

of the small bubble population is clearly demonstrated by the video-imaging experiments carried out be De Swart et al. [31] in a two-dimensional column. The small bubble population is virtually destroyed as the slurry concentration approaches 30 vol.%. This provides an explanation of the significant decrease in the gas hold-up with increasing slurry concentration as observed in Fig. 4.

Data on the gas hold-up in the dense (small bubbles) and dilute (large bubble) phases are shown in Figs. 7 and 8 for the 0.38-m-diameter column. Fig. 7 shows that the dense

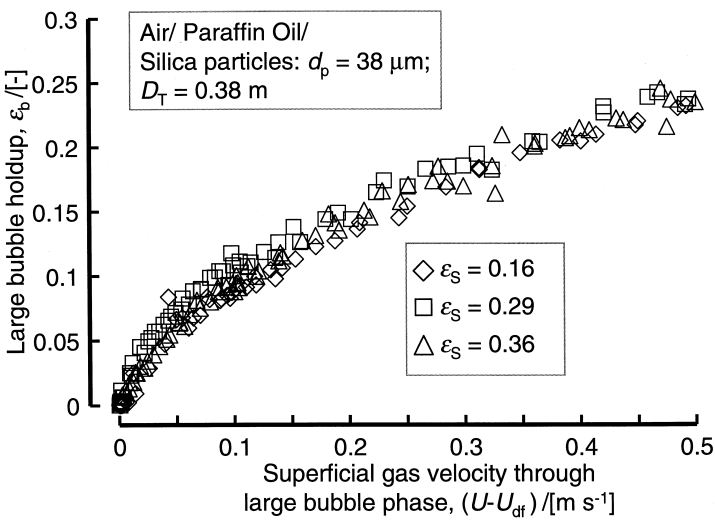

Fig. 8. Large bubble gas hold-up in 0.38-m-diameter column for various slurry concentrations. The experimental data is from Krishna et al. [33]. The system properties are as given in the legend to Fig. 4.

phase gas hold-up is approximately constant for churn–turbulent operation at superficial gas velocities exceeding about 0.1 m/s. This is a useful conclusion for scale-up purposes. Furthermore, we note from the data in Fig. 8 that the large bubble gas hold-up ε_b is practically independent of slurry concentration in the range $0.16 < \varepsilon_s < 0.36$. Fig. 9a shows the collection of data on the gas hold-up in the dense phase, ε_{df}, for all column diameters and slurry concentrations [33]. We see that the dense phase gas hold-up, ε_{df}, is virtually independent of the column diameter and is a significant decreasing function of the particle concentration ε_s. The unique dependence of the decrease in the dense phase gas voidage ε_{df} with increasing solids volume fraction ε_s is useful for scale-up purposes because this parameter can be determined in a relatively

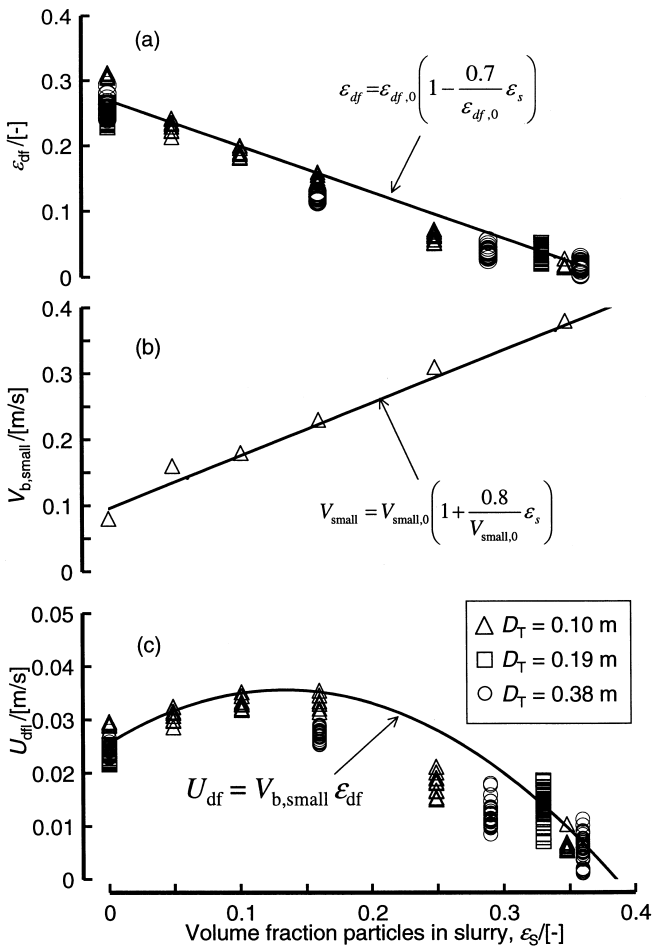

Fig. 9. Influence of particles concentration ε_s on (a) dense phase gas voidage, ε_{df}, (b) rise velocity of the small bubbles, V_{small}, and (c) superficial gas velocity through the dense phase U_{df}. The experimental data is from Krishna et al. [33]. The system properties are as given in the legend to Fig. 4.

small diameter column under actual reaction conditions of temperature and pressure. It is clear that addition of silica particles has the effect of reducing the small bubble population virtually to zero when the slurry concentration approaches 40 vol.%. The addition of solid particles tends to promote the coalescence of small bubbles and the rise velocity of the small bubbles, V_{small}, increases with increasing ε_s (see Fig. 9b). The paraffin oil slurry data on the dense phase voidage ε_{df} and the small bubble rise velocity, V_{small}, can be correlated as:

$$\varepsilon_{df} = \varepsilon_{df,0}\left(1 - \frac{0.7}{\varepsilon_{df,0}}\varepsilon_s\right); \quad V_{small} = V_{small,0}\left(1 + \frac{0.8}{V_{small,0}}\varepsilon_s\right), \tag{1}$$

where the paraffin oil parameters $\varepsilon_{df,0} = 0.27$ and $V_{small,0} = 0.095$ m/s. The superficial gas velocity through the dense phase (see Fig. 6) can be estimated from $U_{df} = V_{small}\varepsilon_{df}$.

4.2. Influence of column diameter on the large bubble (dilute phase) hold-up

As observed in Fig. 8, for slurry concentrations, $\varepsilon_s > 0.16$, the large bubble hold-up, ε_b, remains practically independent of the slurry concentration. This is again a useful scale-up rule. However, the large bubble hold-up is reduced significantly with increasing column diameter (see Fig. 10a). This reduction in the large bubble hold-up is due to the fact that the rise velocity of the large bubbles, V_b, defined by

$$V_b \equiv (U - U_{df})/\varepsilon_b, \tag{2}$$

is higher in a column of larger diameter due to reduced ''wall'' effects. The influence of the ''wall'' is dependent on the ratio of the bubble diameter to column diameter d_b/D_T. Krishna et al. [38] developed a model to describe the large bubble rise velocity by

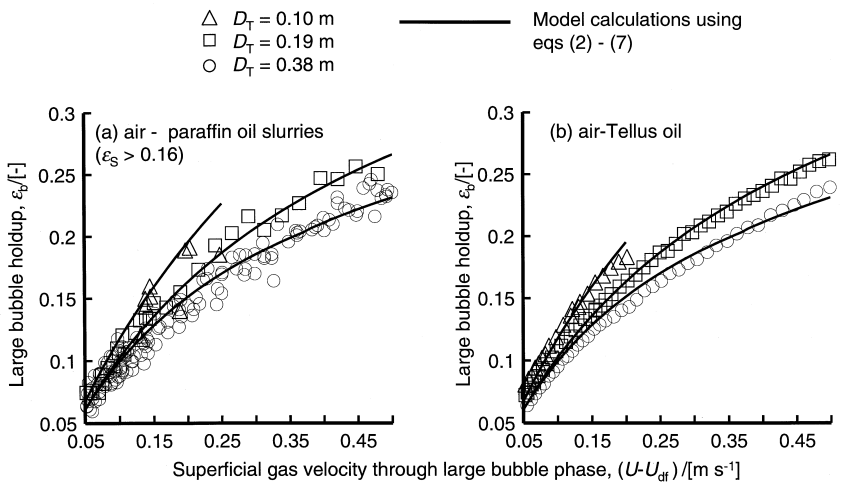

Fig. 10. Influence of column diameter on the hold-up of large bubbles ε_b in (a) paraffin slurries and (b) Tellus oil. Experimental data [33,38] compared with predictions of model using Eqs. (2)–(7).

introducing two correction factors into the classical Davies–Taylor [45] relation for the rise of a single spherical cap bubble in an infinite volume of liquid

$$V_b = 0.71\sqrt{gd_b}\,(\mathrm{SF})(\mathrm{AF}). \tag{3}$$

The scale correction factor (SF) accounts for the influence of the column diameter and is taken from the work of Collins [46] to be

$$\begin{aligned} &\mathrm{SF} = 1 \qquad \text{for } d_b/D_T < 0.125 \\ &\mathrm{SF} = 1.13\exp(-d_b/D_T) \qquad \text{for } 0.125 < d_b/D_T < 0.6 \\ &\mathrm{SF} = 0.496\sqrt{D_T/d_b} \qquad \text{for } d_b/D_T > 0.6. \end{aligned} \tag{4}$$

The acceleration factor, AF, accounts for the increase in the large bubble velocity over that of a single, isolated, bubble; this acceleration is due to wake interactions. This factor increases as the distance between the large bubbles decreases. Since the average distance between large bubbles will decrease as the superficial gas velocity through the large bubble phase increases, we postulate a linear relation for AF:

$$\mathrm{AF} = \alpha + \beta(U - U_{df}), \tag{5}$$

and a power-law dependence of the bubble size on $(U - U_{df})$:

$$d_b = \gamma(U - U_{df})^{\delta}. \tag{6}$$

The model parameters α, β, γ, and δ, were determined by multiple regression for a highly viscous Tellus oil ($\rho_L = 862$; $\mu_L = 0.075$; $\sigma = 0.028$) to be [38]:

$$\alpha = 2.25; \quad \beta = 4.09; \quad \gamma = 0.069; \quad \delta = 0.376. \tag{7}$$

The Eqs. (2)–(7), developed by Krishna et al. [38] for air–Tellus oil is equally valid for air–paraffin oil slurry systems (compare Fig. 10a and b). The equivalence between the hydrodynamics of slurry bubble columns and of bubble columns with high viscous liquids is a useful one, which will be used later to estimate the liquid phase backmixing characteristics.

The above model developed for the large bubble hold-up is adequate for scale-up slurry bubble columns operating at ambient pressure conditions. For high-pressure operation, the model needs to be modified as discussed below.

4.3. Influence of elevated pressure on the gas hold-up in bubble columns

The model developed in Section 4.2 for the large bubble hold-up is adequate for scaling up slurry bubble columns operating at ambient pressure conditions. On the right of Fig. 3 is a schematic representation of the influence of elevated pressure on the gas hold-up. The influence of elevated pressure operation is very significant, as is evidenced by examining the experimental results of Letzel et al. [34] for gas hold-up measured in a bubble column of 0.15 m diameter with the system nitrogen–water (see Fig. 11a). For example, for operation at a superficial gas velocity $U = 0.2$ m/s, the gas hold-up, ε,

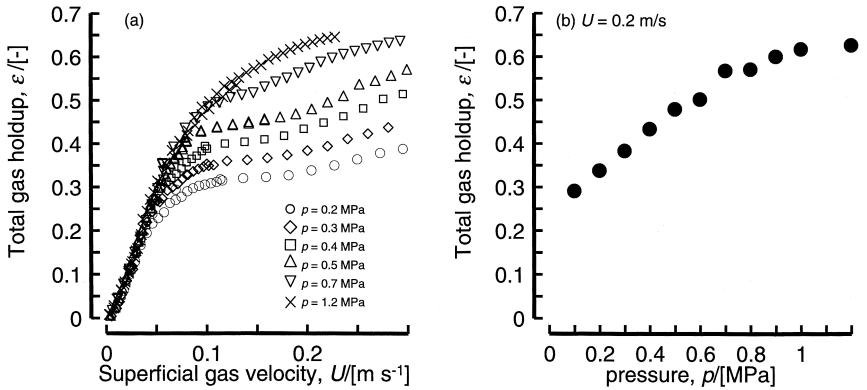

Fig. 11. Experimental data of Letzel et al. [34,35,40] describing the influence of elevated pressure on gas hold-up.

can increase from a value of 0.29 at $p = 0.1$ MPa to a value, which is twice as large for operation at $p = 1.2$ MPa (see Fig. 11b).

Increased system pressure influences (a) the regime transition point, (b) the gas voidage at the regime transition point, and (c) the large bubble hold-up. We discuss these below.

Several workers [27,43,47,48] have shown that with increased system pressure, the gas hold-up at the transition point, ε_{trans}, increases. The correlation of Reilly et al. [47] for ε_{trans}:

$$\varepsilon_{trans} = 0.59 B^{1.5} \sqrt{\rho_G^{0.96} \sigma^{0.12} / \rho_L}\,, \tag{8}$$

is adequate for estimation purposes. The parameter $B = 3.85$. Eq. (8) has been developed for ''pure'' liquids and is recommended when no experimental data is available. When comparing Eqs. (1) and (8) we note that the influence of increasing system pressure (or equivalently, increasing gas density) and increasing catalyst concentration on the dense phase voidage, act in opposing ways. The influence of increased system pressure on the dense phase gas voidage in slurry systems can be obtained by combining Eqs. (1) and (8) to obtain

$$\varepsilon_{df} = \varepsilon_{df,0} \left(\frac{\rho_G}{\rho_{G,ref}} \right)^{0.48} \left(1 - \frac{0.7}{\varepsilon_{df,0}} \varepsilon_s \right), \tag{9}$$

where $\rho_{G,ref}$ is the density of gas at ambient conditions ($= 1.29$ kg/m^3 in usual experimental work with air at atmospheric pressure as the gas phase).

In pure liquids, the ''small'' bubble rise velocity, $V_{small,0}$, is only very weakly dependent on the gas density; this rise velocity is best determined experimentally. The superficial gas velocity through the dense phase, $U_{df} = V_{small} \varepsilon_{df}$, for slurry systems at elevated pressures can be calculated by combining Eqs. (1) and (8).

A more recently published effect of elevated pressure is that the large bubbles become less stable [35]. To account for this, we introduce a further gas density correction factor, DF, into Eq. (3):

$$V_b = 0.71\sqrt{gd_b}\,(\mathrm{SF})(\mathrm{AF})(\mathrm{DF}). \tag{10}$$

Using the Kelvin–Helmholtz stability theory as basis, Letzel et al. [35] concluded that this correction factor is inversely proportional to the square root of the gas density. For air at atmospheric conditions used in the experiments, $\rho_G = 1.29$ kg/m^3 and the density correction factor is unity, i.e., DF = 1. For any gas at any system pressure, having a gas density ρ_G, the density correction factor can be calculated from

$$\mathrm{DF} = \sqrt{1.29/\rho_G}\,. \tag{11}$$

The FT synthesis of hydrocarbons in a bubble column slurry reactor using synthesis gas, a mixture of CO and H_2, is carried out at a pressure in the range of about 30 MPa. The syngas density at this pressure is 7 kg/m^3 and the large bubble rise velocity at these conditions is only a fraction $\sqrt{1.29/7} = 0.43$ of the velocity it would have in cold-flow experiments carried out under atmospheric pressure conditions with air as the gas phase. This underlines the importance of the density correction factor developed above.

The modification given by Eqs. (10) and (11), can be introduced into the Eqs. (1)–(7) for estimation of the large bubble hold-up in slurry bubble columns operated at elevated pressures. Following the model of Krishna and Ellenberger [32] for churn–turbulent regime operation, the total gas hold-up can be determined as follows:

$$\varepsilon = \varepsilon_b + \varepsilon_{df}(1 - \varepsilon_b). \tag{12}$$

The dense phase gas hold-up, ε_{df}, remains roughly constant in the churn–turbulent regime (see Fig. 7).

4.4. Mass transfer

Due to the small size of catalyst particles in slurry reactors (particle diameter typically of the order of 50 μm), intraparticle diffusion is not a limiting factor. With catalysts of relatively low activity present in low concentration in bubble columns, operated in the homogeneous regime, gas–liquid mass transfer is unlikely to be a limiting factor either in view of the large surface area of the small bubbles and their long residence time in the liquid. However, for reactors of increased productivity because of the use of more active catalysts in high concentrations and operation in the heterogeneous regime, gas–liquid mass transfer becomes a factor that needs serious consideration. Conventional calculation of mass transfer rates, based on the application of the surface renewal theory with the hold-up and the size of the large bubbles (which represent the major part of the gas throughput) as input, yields relatively low rates, which would considerably detract from the attractiveness of bubble columns as FT reactors. Experimental data, obtained on model systems, would seem to suggest that the situation is not as bleak, however, since actual rates are found to be higher than the calculated ones by a factor of 5–10. Experimental gas–liquid mass transfer rates for turpentine–nitrogen in the heterogeneous regime were found to be an order of magni-

tude higher than the estimated on the basis of correlations that have been established for small bubbles mainly [26].

Letzel et al. [40] measured the volumetric mass transfer coefficient $k_L a$ for the air–water system at various system pressures. Their experimental data (see Fig. 12) showed that the whole data set could be approximated by the simple relation

$$\frac{k_L a}{\varepsilon} \approx 0.5 \tag{13}$$

for both homogeneous and heterogeneous regimes of operation. The relation (13), which stems from the early work of Vermeer and Krishna [26], implies that there is no detrimental effect accruing from operation in the heterogeneous flow regime. This appears to be paradoxical at first sight because for heterogeneous regime of operation, one observes bubbles of about 50 mm in size, an order of magnitude larger than in the homogeneous flow regime.

An explanation for this paradox was obtained in work of De Swart et al. [31], using high speed video imaging techniques to study the dynamics of large bubbles in concentrated slurries. In these studies, it was observed that within the class of large bubbles, bubbles of a given size do not lead an isolated life, but are continually disappearing and reappearing as a result of break-up and coalescence. De Swart et al. [31] determined that the exchange of gas between various bubble classes occurs at a very high rate, at least 4 s^{-1}, which is higher than the characteristic renewal rate for mass transfer. Put another way, during the characteristic time for mass transfer from the gas to the liquid phase, a bubble loses its identity because of frequent exchange with gas in other bubble size classes. Thus, whereas the gas throughput is mainly represented by the

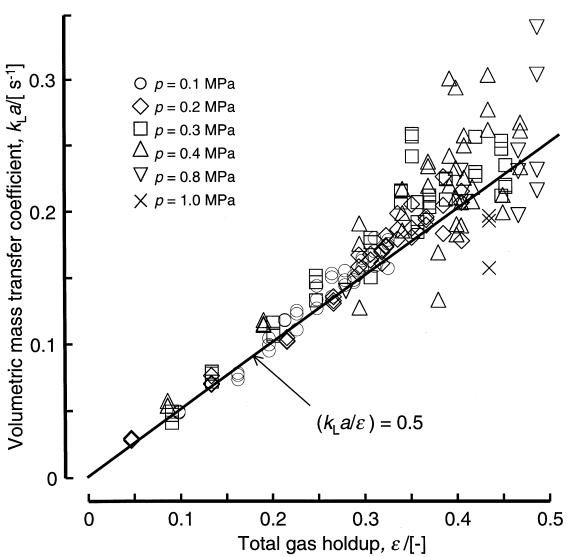

Fig. 12. Data on volumetric mass transfer coefficient $k_L a$ obtained by Letzel et al. [40] at various system pressures for the air–water system in a 0.15-m-diameter column.

largest bubbles, gas–liquid mass transfer is largely determined by the interfacial area of the smaller bubbles. In other words, the equivalent bubble size, regarded as mass transfer is relatively small and small enough for mass transfer not to be a limiting factor in FT synthesis in most cases.

For a bubble column reactor, operating with concentrated slurry in the heterogeneous flow regime at elevated pressures, the relation (13) can be applied after applying two corrections. Firstly, the total gas hold-up is predominantly made up of large bubbles, and so $\varepsilon \approx \varepsilon_b$. Secondly, the mass transfer coefficient needs to be corrected for the liquid phase diffusivity under the actual conditions prevailing in the FT reactor.

$$\frac{k_L a}{\varepsilon_b} = 0.5\sqrt{\frac{\bar{D}_L}{\bar{D}_{L,ref}}}, \tag{14}$$

where $\bar{D}_L$ is the diffusion coefficient in the liquid phase, while $\bar{D}_{L,ref}$ is equal to 2×10^{-9} m^2/s (valid for the measurement systems in Vermeer and Krishna [26]). The diffusivities, $\bar{D}_L$, of the CO and H_2 species at a reaction temperature of, say, 240°C, are 17.2×10^{-9} and 45.5×10^{-9} m^2/s, respectively.

4.5. Backmixing of the ''dense'' phase

For churn–turbulent regime operation, the large bubbles tend to concentrate near the centre of the column and carry liquid (slurry) upwards in their wake. At the top of the dispersion, the large bubbles disengage and the liquid (slurry) is re-circulated. Fig. 13a shows the measured radial liquid velocity distribution $V_L(r)$ for the three columns operating at a superficial gas velocity of 0.23 m/s with the air–water system. The strong influence of the column diameter is evident. We note the strong downwardly directed liquid velocity in the wall region and the upwardly directed velocity in the central core. This liquid re-circulation is the cause of liquid phase dispersion and backmixing. If all the measured $V_L(r)$ data for air–water systems are normalised with respect to the centre line velocity, $V_L(0)$, we see that the radial distributions are all similar (see Fig. 13b). The important conclusion that can be drawn from the result in Fig. 13 is that the magnitude of re-circulatory flows can be characterised by a single velocity, the centre-line liquid, $V_L(0)$. This would suggest that the liquid phase dispersion coefficient $D_{ax,L}$ should be proportional to $V_L(0)$. Of the literature correlations, we consider the one due to Riquarts [49]:

$$V_L(0) = 0.2(gD_T)^{1/2}\left(U^3/g\nu_L\right)^{1/8}, \tag{15}$$

as most suitable for estimation purposes. The Riquarts correlation (15) anticipates a dependence of $V_L(0)$ on the kinematic viscosity of the liquid phase, ν_L. However, the experimental data of Urseanu [39] shows that the liquid viscosity has a negligible influence on the centre-line velocity $V_L(0)$ and the radial distribution $V_L(r)$ (see Fig. 14). We therefore recommend the use of Eq. (15) for all systems (including slurries!) taking $\nu_L = 10^{-6}$ m^2/s.

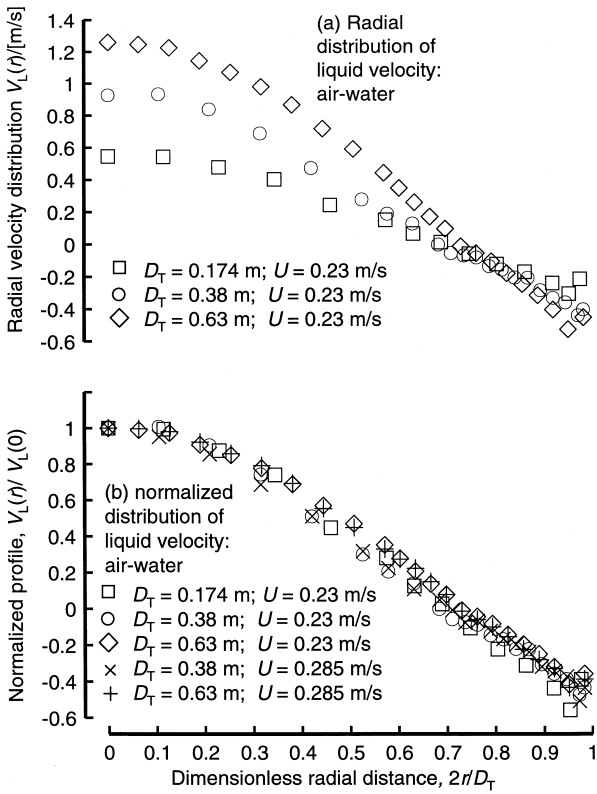

Fig. 13. (a) Radial distribution of the axial component of the liquid velocity at a superficial gas velocity $U = 0.23$ m/s for three column diameters with the air–water system. (b) Normalized radial velocity distribution profiles for air–water system. Measurements of Urseanu [39] and Krishna et al. [41].

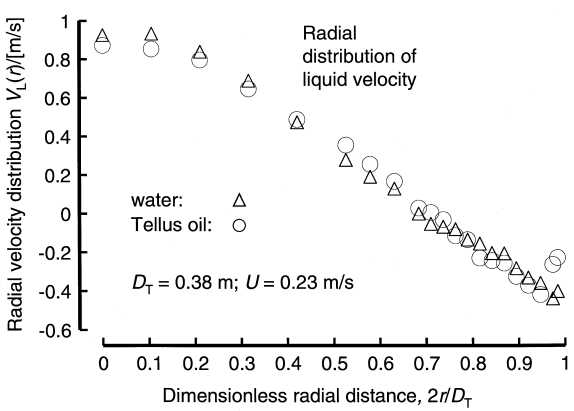

Fig. 14. Radial distribution of the axial component of the liquid velocity at a superficial gas velocity $U = 0.23$ m/s for air–water and air–Tellus oil system measured in a 0.38-m-diameter column. Measurements of Urseanu [39].

From the results of Fig. 10, we have established that the hydrodynamics of concentrated slurry columns are equivalent to that of highly viscous Tellus oil. In Fig. 14, we see that as far as radial distribution of liquid velocity is concerned, the air–Tellus oil system is analogous to that of an air–water system when compared at the same superficial gas velocity. The remarkable conclusion to be drawn from (Figs. 10, 13, and 14), is that the slurry phase backmixing is the same as for low viscosity liquids, such as water. Measured experimental data [41,50–53] for the liquid phase axial dispersion coefficient $D_{ax,L}$ show that this parameter is a simple product of the centre-line liquid velocity $V_L(0)$ and column diameter D_T:

$$D_{ax,L} = 0.31 V_L(0) D_T, \tag{16}$$

where we take Eq. (15), using the kinematic viscosity of water at room temperature, for the estimation of $V_L(0)$, as can be seen in Fig. 15.

For a commercial scale bubble column slurry reactor of diameter $D_T = 7$ m operating at $U = 0.35$ m/s, Eqs. (15) and (16) yield an estimate of $D_{ax,L} = 10$ m^2/s, suggesting that the ''dense'' phase can be considered to be well-mixed.

4.6. Heat transfer in bubble columns

The effective heat transfer and the good temperature equalisation in a slurry bubble column, particularly when operated in the heterogeneous regime, are important advantages of this type of reactor. Heat transfer coefficients in the region of 1000 W m^{-2} K^{-1} can be obtained as can be seen from the estimations in Fig. 16, which are based on the Deckwer et al. [54] correlation, adapted to take more recent insights into slurry column hydrodynamics. It can be seen that the heat transfer coefficient increases with increasing gas velocity and with increasing solids concentration, i.e., with factors, which favour the heterogeneous regime.

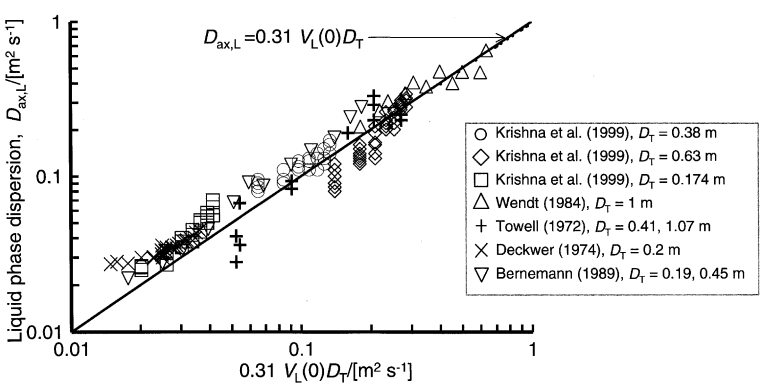

Fig. 15. Axial dispersion coefficient of the liquid phase. Comparison of experimental data [39,41,50–53] with the correlation $D_{ax,L} = 0.31 V_L(0) D_T$, wherein the centre-line liquid velocity is estimated from the Riquarts correlation (15) taking $\nu_L = 10^{-6}$ m^2/s.

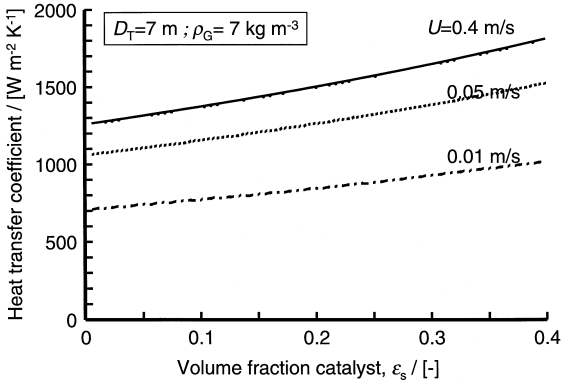

Fig. 16. Estimate of the heat transfer coefficients to vertical cooling tubes. The estimations are based on the correlation of Deckwer et al. [54].

4.7. Operational aspects

There are several operational aspects of bubble column slurry reactors that deserve attention.

(A) Catalyst loading and unloading in bubble column slurry reactors is much easier than in multi-tubular fixed-bed reactors and can be accomplished in a shorter time. Moreover, the activity of the catalyst inventory in the reactor can be maintained by the withdrawal of catalyst and replacement with fresh catalyst during a run.

(B) In the case of the synthesis of heavy FT products, separation of solids from the liquid in the slurry reactor technology may not be a trivial problem. Distilling off the product is not possible with heavy liquids, and filtering may prove to be necessary. The separation problem is aggravated if fines are produced by catalyst attrition (either mechanical or chemical attrition).

(C) Foam formation is obviously a problem to be avoided in a bubble column FT reactor.

(D) At too low velocities, a concentration gradient of catalyst may develop in a slurry reactor and this may limit the turndown ratio. Deposition of insoluble, sticky material onto the catalyst particles may hamper proper suspension of the catalyst.

5. Modelling and optimisation of FT slurry reactor

The information presented above on the design parameters for a bubble column slurry reactor has been incorporated into a reactor model for the purposes of design and optimisation of FT slurry reactors by Van der Laan et al. [42] and Maretto and Krishna [44], using, Fe and Co catalysts, respectively. The simulation results of Maretto and Krishna [44] for a commercial scale reactor with diameter $D_T = 7$ m operating at a pressure of 3 MPa and temperature $T = 513$ K are discussed in some detail below. For the purposes of property estimation, the liquid phase is taken to be $C_{16}H_{34}$. The details

Table 1
Operating conditions and system properties for commercial Fischer–Tropsch slurry bubble column

Operating Conditions	
Reactor temperature	$T = 513$ K
Reactor pressure	$P = 3$ MPa
Reactor diameter	$D_T = 7$ m
Slurry dispersion height	$H = 30$ m
Diameter of cooling tubes placed vertically	$d_t = 50$ mm
Height of vertical cooling tubes	$H = 30$ m
Temperature of coolant	$T_w = 503$ K
Liquid phase properties	
Density	$\rho_L = 640$ kg/m^3
Viscosity	$\mu_L = 0.00029$ Pa s
Surface tension	$\sigma = 0.01$ N m
Thermal conductivity	$\lambda_L = 0.113$ W/m/K
Heat capacity	$C_{p,L} = 1500$ J/kg/K
Diffusivity of H_2	$\bar{D}_{H_2,L} = 45.5\times10^{-9}$ m^2/s
Diffusivity of CO	$\bar{D}_{CO,L} = 17.2\times10^{-9}$ m^2/s
Distribution coefficient for H_2	$m = 2.96$; $c_G^* = mc_L$
Distribution coefficient for CO	$m = 2.48$; $c_G^* = mc_L$
Properties Co/MgO catalyst (21.4 wt.% Co and 3.9 wt.% Mg) supported on silica	
Particle diameter	$d_p = 50$ μm
Particle density	$\rho_p = 647$ kg/m^3
Pore volume	$V_o = 0.00105$ m^3/kg
Skeleton density	$\rho_{SK} = 2030$ kg/m^3
Thermal conductivity	$\lambda_s = 1.7$ W m^{-1} K^{-1}
Heat capacity	$C_{p,s} = 992$ J kg^{-1} K^{-1}

of the operating conditions, as well as the liquid and catalyst properties are listed in Table 1. For the chosen reactor dimensions, the liquid phase can be considered to be well-mixed and the conditions will be practically isothermal. The catalyst is expected to be well dispersed in the liquid and there will be no solids gradient along the reactor height. Such gradients can be expected only in tall narrow pilot plant reactors with small diameters of, say, 0.1–0.2 m. Syngas with a molar ratio $H_2/CO = 2$ enters the reactor. The appropriate reactor model, which emerges from the hydrodynamic studies described in Section 4, is shown in Fig. 17. The large bubbles are assumed to traverse the column in plug flow with a superficial gas velocity of $U - U_{df}$, where U_{df} is the superficial gas velocity through the small bubbles. The properties of the slurry were determined using the recommendations of Deckwer [54].

The Yates and Satterfield kinetics [55] for the reaction rate of CO for the FT synthesis reaction scheme: $CO + 2H_2 \rightarrow -CH_2- + H_2O$ is given by

$$-R_{CO} = \frac{ap_H\, p_{CO}}{(1 + bp_{CO})^2}, \tag{17}$$

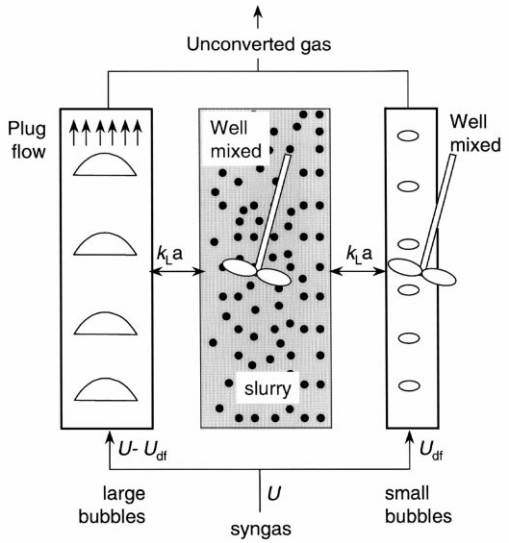

Fig. 17. Calculation model of the Fischer–Tropsch slurry reactor [44]. The stirrers shown are only symbolic and denote well-mixed characteristic of the small bubbles and slurry phases.

where R_{CO} is the consumption rate of CO expressed in mole CO per kilogram of supported Co/MgO catalyst per second,

$$a = 8.8533 \times 10^{-3} \exp\left[4494.41\left(\frac{1}{493.15} - \frac{1}{T}\right)\right] \text{mol s}^{-1}\,\text{kg}_{\text{cat}}^{-1}\,\text{bar}^{-2} \tag{18}$$

and

$$b = 2.226 \times \exp\left[-8236\left(\frac{1}{493.15} - \frac{1}{T}\right)\right] \text{bar}^{-1}. \tag{19}$$

A simpler first order kinetics, like the one proposed by Post et al. [56] for a zirconium-promoted cobalt catalyst on silica support has been incorporated in various other reactor models for FT synthesis slurry bubble column reactors [57]. However, the Yates–Satterfield kinetics is more realistic than that of the Post et al. [56], when operating at high syngas conversion (above 60%) and when the H_2/CO feed ratio is close to the stoichiometric ratio (i.e., when H_2 is not the limiting species). For cobalt catalyst with negligible water–gas shift activity, the H_2/CO stoichiometric ratio is nearly 2.

It is must be underlined that the Yates–Satterfield kinetics were determined for a narrow temperature range of 220–240°C, and hydrocarbon selectivity was not included in their model. To describe the catalyst selectivity, the Anderson–Schulz–Flory for the carbon number distribution was chosen. Considering that most of the hydrocarbon products are paraffins, the mole fraction of each species C_nH_{2n+2} is obtained as follows $x_n = (1 - \alpha_{ASF})\,\alpha_{ASF}$, where α_{ASF} is the probability factor of hydrocarbon chain growth. The higher the α_{ASF} factor, the higher is the fraction of heavy paraffins. A

value of $\alpha_{ASF} = 0.9$ is chosen as a typical value for the Co catalyst. The consumption ratio of CO and H_2 is 2. As the feed ratio of CO and H_2 was set equal to the consumption ratio, the conversion of CO and H_2 are both equal to one another, χ_{CO+H}. The amount of inerts in the entering gas phase was taken to be 5% and the gas contraction factor (for 100% syngas conversion) can be calculated as $\phi = -0.48$. The superficial gas velocity varies with conversion as $U(1 + \phi\chi_{CO+H})$.

For the removal of reaction enthalpy $\Delta H = -170$ kJ/(mol CO), vertical cooling tubes of 50 mm diameter are installed with a constant coolant (steam) temperature of 230°C. The heat transfer coefficient from slurry to the coolant was estimated as shown in Fig. 16. The pitch for the vertical cooling tubes will depend on the number of tubes to be installed. In the calculations, the pitch varied from 0.12 to 0.19 m. This pitch size is considered to be large enough not to influence the bubble size, the bubble hold-up, or the slurry phase backmixing. Simulations based on the reactor model shown in Fig. 17 were carried out for a range of superficial gas velocities $U = 0.12 - 0.4$ m/s, while the catalyst concentration range was $\varepsilon_s = 0.20–0.35$. The main results of the simulations are reported in Figs. 18–20.

Increasing the inlet superficial gas velocity causes a decrease in the conversion of the gas phase (Fig. 18), while reactor productivity increases (Fig. 19), and so does the number of tubes necessary to remove the heat produced by the synthesis reaction (Fig. 20). For example, for the case where $\varepsilon_s = 0.30$, while conversion changes from 96% at the lower gas velocity, to 63% at the higher, the productivity of the reactor increases from 1200 to 2640 $tons_{Cl+}$/day and the required number of cooling tubes increases from 2700 to 5900. In this case, it is evident that, at the highest reactor productivity, the conversion of syngas is not complete, and the non-reacted syngas should be recycled to the reactor or passed on to a reactor in a next stage. In practice, it is desirable to operate at conversion levels of about 90% per single pass avoiding the recycle of the gas phase. Therefore, it is necessary to operate at superficial gas velocities below 0.3 m/s (see Fig. 18).

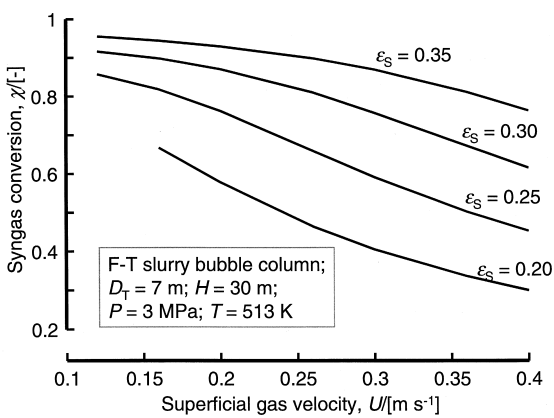

Fig. 18. Fischer–Tropsch reactor simulation results [44]: syngas conversion.

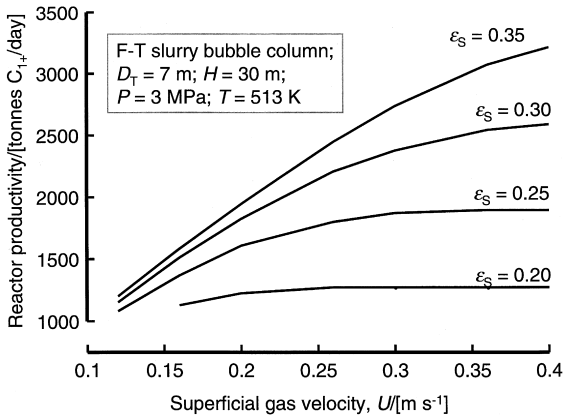

Fig. 19. Fischer–Tropsch reactor simulation results [44]: total reactor productivity (column diameter $D_T = 7$ m; dispersion height $H = 30$ m).

Increasing the slurry concentration, ε_s, increases the conversion and the reactor capacity, as well as the number of required cooling tubes to be installed in the reactor. The influence of ε_s is not only on the kinetic term, which is proportional to the catalyst loading, but also on the total gas hold-up. Increasing ε_s reduces the total gas hold-up, making more room available for the catalyst. Therefore, increasing ε_s has more than a proportional influence on the reactor conversion and productivity. From the reactor performance point of view, it is advisable to use the highest catalyst concentrations consistent with ease of handleability. We consider $\varepsilon_s = 0.40$, the maximum slurry concentration, which can be used in commercial practice.

An economically viable FT complex would need to have a high production capacity, of the order of 5000 tons/day of middle distillates, which can be considered to be C_{10+} hydrocarbon products. For the assumed Anderson–Schultz–Flory distribution with the

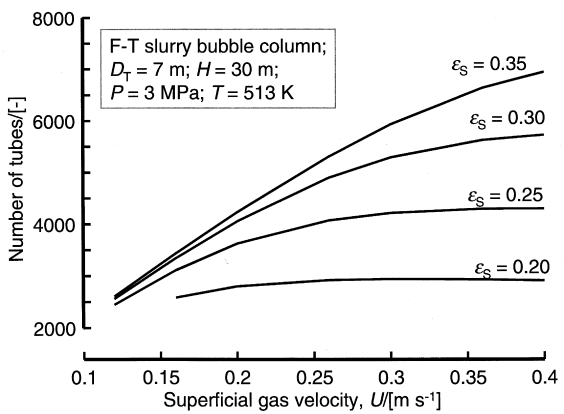

Fig. 20. Fischer–Tropsch reactor simulation results [44]: number of 50-mm-diameter cooling tubes.

probability chain growth factor $\alpha_{ASF} = 0.9$, we estimate that 80% of the C_{5+} products will be in the middle distillates range. From the results presented in Fig. 19, we find that operation at a superficial gas velocity at the inlet of 0.3 m/s and a slurry concentration of 35 vol.% would require a total of three reactors in parallel in order to produce 5000 tons/day of middle distillates. Three reactors allow a good degree of flexibility on operating conditions. In each of these three reactors, we would need to install about 6000 vertical cooling tubes at a pitch of about 0.15 m.

Increasing or decreasing the interphase mass transfer coefficient from the base case value has a negligible effect on reactor performance. Increasing the Yates–Satterfield kinetic parameter *a* by a factor of 2 results in a 60% increase in reactor productivity. It can be concluded that the FT reactor is kinetically controlled. If the catalyst activity is twice as high as given by Yates–Satterfield, then the number of reactors in parallel required for a 5000 tons/day middle distillates complex will be two, instead of three. The importance of improved catalyst formulations in developing a viable FT reactor technology is evident.

The model calculations presented in Figs. 18–20, are best estimates based on cold-flow experimental studies. In order to avoid costly failures on a commercial scale, it is often considered necessary to build a ''hot'' demonstration unit for purposes of validating the scaling rules and gaining operating experience. For example, a demonstration reactor with a diameter of 1.2 m in a 21-m-high structure has been erected in 1990 at Exxon's R&D laboratory at Baton Rouge, LA, US. However, with improved insight into the fundamentals of the hydrodynamics and scale rules of slurry bubble columns, coupled with increased practical experience on the operation and performance of industrial slurry FT reactor, the need for the construction and operation of costly ''hot'' demonstration units will diminish in the future. The ultimate ideal would be the reliable design of an industrial slurry FT reactor based solely on catalytic and process data generated in relatively small ''hot'' process development units (bench-scale or small pilot plant reactors), which are linked to hydrodynamic information via a computational reactor model.

6. Conclusions

The recently developed FT reactors of the gas–solid fluidised-bed, multi-tubular trickle-bed, and slurry bubble column type, have considerably larger production capacities than the classical ones: commercial reactors of all three types have been built with capacities of 2500 bbl/day or higher, which is more than two orders of magnitude higher than that of the commercial reactors operated before and during World War II. The gas–solid fluidised reactor is restricted to the synthesis of products characterised by a growth chance parameter α_{ASF} of less than 0.7, and is therefore, only applicable if gasoline is the target product. The multi-tubular trickle-bed and the slurry bubble column are suited for the production of heavier FT products, such as middle distillates, lubeoils, and waxes. With multi-tubular trickle-bed reactors, intraparticle diffusion limitation plays a role and catalyst particle size and shape should therefore be carefully chosen. For large-scale production, the slurry bubble column is best operated in the

heterogeneous or churn–turbulent regime. Notwithstanding the presence of large diameter bubbles and their short residence time in the liquid, gas–liquid mass transfer is quite fast in this regime due to the effective interaction between bubbles of various sizes.

Whereas the upscaling of the multi-tubular reactor from a pilot plant scale to an industrial scale is relatively straightforward and safe, this is not the case for the bubble column reactor and a costly demonstration stage is generally considered to be necessary. However, recent insights in the hydrodynamics of this reactor suggest that a rational upscaling strategy based on the investigations in small ''hot'' pilot plants and larger ''cold-flow'' engineering test rigs may be adopted as alternative to the traditional, largely empirical development route. Based on the presently available knowledge, it can be expected that a bubble column FT reactor may achieve a productivity of 2500 tons/day (about 20,000 bbl/day), which is a thousand times higher than that of the classical FT reactor operated in the forties.

Besides developments in reactor technology, significant improvements have also been realised in the catalysis of the FT process in recent years. A discussion of the advances in catalysis, which is rendered difficult, because most information is in the domain of proprietary company know-how, is outside the scope of the present paper. However, it will be clear that the combination of advances in catalysis and reactor technology, together with innovations in syngas production, have considerably improved the prospects of large-scale economic production of synthetic hydrocarbons from remote natural gas.

7. Notation

a	Yates–Satterfield reaction rate constant, mol s^{-1} kg_{cat}^{-1} bar^{-2}
AF	wake acceleration factor, dimensionless
b	Yates–Satterfield absorption constant, bar^{-1}
B	constant in Reilly correlation
d_b	large bubble diameter, m
d_p	particle size, m
$D_{ax,L}$	liquid phase axial dispersion coefficient, m^2/s
DF	density correction factor, defined by Eqs. (8) and (9), dimensionless
$\bar{D}_L$	diffusion coefficient in the liquid phase m^2/s
$\bar{D}_{L,ref}$	reference diffusion coefficient in the liquid, m^2/s
D_T	column diameter, m
g	acceleration due to gravity, 9.81 m/s^2
H	dispersion height of the reactor, m
$k_L a$	volumetric mass transfer coefficient, s^{-1}
p	pressure, Pa or bar
r	radial coordinate, m
R_{CO}	CO consumption rate, mol kg_{cat}^{-1} s^{-1}
SF	scale correction factor, dimensionless
T	reactor temperature, K
U	superficial gas velocity, m/s
$(U - U_{df})$	superficial gas velocity through the large bubbles, m/s

U_{df} superficial velocity of gas through the small bubbles, m/s
V_{small} rise velocity of the small bubbles, m/s
$V_{small,0}$ rise velocity of the small bubbles at 0% solids concentration, m/s
$V_L(r)$ radial distribution of liquid velocity, m/s
$V_L(0)$ centre-line liquid velocity, m/s
U_{trans} superficial gas velocity at regime transition, m/s
z axial coordinate, m

Greek letters

$\alpha, \beta, \gamma, \delta$ parameters defined by Eqs. (5) and (6)
α_{ASF} Anderson–Schulz–Flory chain growth probability factor, dimensionless
χ_{CO+H} syngas conversion, dimensionless
ε total gas hold-up, dimensionless
ε_b gas hold-up of large bubbles, dimensionless
ε_{df} gas hold-up of the ''dense phase'', dimensionless
ε_s volume fraction of catalyst in the slurry phase, dimensionless
ε_{trans} gas hold-up at the regime transition point, dimensionless
ϕ gas contraction factor, dimensionless
μ_L liquid viscosity, Pa s
ν kinematic viscosity of phase, m^2/s
ρ_G density of gas phase, kg/m^3
$\rho_{G,ref}$ density of gas phase at atmospheric conditions, kg/m^3
ρ_L liquid density, kg/m^3
σ surface tension of liquid phase, N/m

Subscripts

b referring to large bubbles phase
CO referring to CO species
df referring to small bubbles
G referring to gas phase
H referring to H_2
L referring to liquid phase
large referring to large bubbles
p referring to solid particle
s referring to solids
SL referring to slurry
small referring to small bubbles
trans referring to regime transition point
T tower or column

References

[1] H. Kölbel, Die Fischer–Tropsch Synthese, in: Winnacker-Küchler Chemische Technologie, Organische Technologie I Vol. 3 Karl Hauser Verlag, Munich, 1959, pp. 439–520.
[2] O. Roelen, H. Pichler, W. Rottig, H.W. Gross, H. Kölbel, P. Ackermann, Technik der Kohlenoxyd-Hydrierung, in: 3rd edn., Ullmanns Encyklopädie der Technischen Chemie 9 Urban und Schwarzenberg, Munich, 1957, pp. 704–727.

[3] H. Tramm, Technische und Wirtschaftliche Möglichkeiten der Kohlenoxyd-Hydrierung, Chem. Ing. Tech. 24 (1952) 237–332.
[4] J.C. Hoogendoorn, J.M. Salomon, Sasol: worlds largest oil-from-coal plant, Brit. Chem. Eng., 2, 1957, 238–244; 308–312; 368–373; 418–419.
[5] H. Tramm, Inbetriebnahme der Ruhrchemie/Lurgi Fischer–Tropsch Synthese in Sasolburg (Süd Afrika), Brennst.-Chem. 37 (1956) 117–119.
[6] H. Kölbel, P. Ackermann, F. Engelhardt, Nue Entwicklungen zur Kohlenwasserstoff-Synthese, Erdöl und Kohle, 9, 1956, 153, 225, 303.
[7] H. Kölbel, P. Ackermann, Hydrogenation of carbon monoxide in the liquid phase, in: Proc. 3rd World Petroleum Congress, The Hague 1951, Sect. IV, 1951, pp. 2–12.
[8] H. Kölbel, P. Ackermann, Grosstechnische Versuche zur Fischer–Tropsch Synthese in flüssiger Medien, Chem. Ing. Tech. 28 (1956) 381–388.
[9] H.E. Benson, J.H. Crowell, J.H. Field, H.H. Storch, US Bureau of Mines Fischer–Tropsch pilot plant, in: Studies of oil circulation process, Proc. 3rd World Petroleum Congress, The Hague 1951, 1951, pp. 39–55.
[10] H.E. Benson, J.H. Field, D. Bienstock, H.H. Storch, Oil circulation process for Fischer–Tropsch synthesis, Ind. Eng. Chem. 46 (1954) 2278–2285.
[11] J.H. Crowell, H.E. Benson, J.H. Field, H.H. Storch, Fischer–Tropsch oil circulation processes, Ind. Eng. Chem. 42 (1950) 2376–2384.
[12] P.C. Keith, Gasoline from natural gas, Oil Gas J. 45 (1946) 102–112, (June).
[13] L.W. Garrett Jr., Gasoline from coal via the Synthol process, Chem. Eng. Prog. 56 (1960) 39–41.
[14] B. Jager, Developments in Fischer–Tropsch Technology, Stud. Surf. Sci. Catal. 107 (1997) 219–224.
[15] S.T. Sie, Process development and scale-up: Part 4. Case history of the development of a Fischer–Tropsch synthesis, Rev. Chem. Eng. 14 (1998) 109–157.
[16] S.T. Sie, R. Krishna, Process development and scale-up: Part 2. Catalyst design strategy, Rev. Chem. Eng. 14 (1998) 159–202.
[17] D. Bode, S.T. Sie, Neth. Pat. Appl. 8500121, 18 Jan. 1985, assigned to Shell Internationale Research Mij
[18] B. Jager, R.C. Kelfkens, A.P. Steynberg, A slurry bed reactor for low-temperature Fischer–Tropsch, Stud. Surf. Sci. Catal. 81 (1994) 419–425.
[19] B. Jager, R. Espinoza, Advances in low temperature Fischer–Tropsch synthesis, Catal. Today 23 (1995) 17–28.
[20] B. Eisenberg, R.A. Fiato, C.H. Mauldin, G.R. Say, S.L. Soled, Exxon's advanced gas-to-liquids technology, Stud. Surf. Sci. Catal. 119 (1998) 943–948.
[21] B.M. Everett, B. Eisenberg, R.F. Baumann, Advanced gas conversion technology: a new option for natural gas development, in: First Doha conference on natural gas, 14 March 1995, Doha, Qatar, 1995.
[22] http://www.sasol.com/.
[23] J.W.A. de Swart, R. Krishna, S.T. Sie, Selection, design and scale-up of the Fischer–Tropsch reactor, Stud. Surf. Sci. Catal. 107 (1997) 213–218.
[24] W.D. Deckwer, Bubble Column Reactors, Wiley, New York, 1992.
[25] L.S. Fan, Gas–liquid–solid fluidization engineering, Butterworth, Boston, 1989.
[26] D.J. Vermeer, R. Krishna, Hydrodynamics and mass transfer in bubble columns operating in the churn–turbulent regime, Ind. Eng. Chem. Process Des. Dev. 20 (1981) 475–482.
[27] R. Krishna, P.M. Wilkinson, L.L. Van Dierendonck, A model for gas hold-up in bubble columns incorporating the influence of gas density on flow regime transitions, Chem. Eng. Sci. 46 (1991) 2491–2496.
[28] R. Krishna, J. Ellenberger, D.E. Hennephof, Analogous description of gas–solid fluidized beds and bubble columns, Chem. Eng. J. 53 (1993) 89–101.
[29] R. Krishna, J. Ellenberger, A unifed approach to the scale-up of ''fluidized'' multiphase reactors, Chem. Eng. Res. Des. (Trans. Inst. Chem. Eng.) 73 (1995) 217–221.
[30] R. Krishna, J. Ellenberger, S.T. Sie, Reactor development for conversion of natural gas to liquid fuels: a scale-up strategy relying on hydrodynamic analogies, Chem. Eng. Sci. 51 (1996) 2041–2050.
[31] J.W.A. de Swart, R.E. van Vliet, R. Krishna, Size, structure, and dynamics of ''large'' bubbles in a 2-D slurry bubble column, Chem. Eng. Sci. 51 (1996) 4619–4629.
[32] R. Krishna, J. Ellenberger, Gas hold-up in bubble column reactors operating in the churn–turbulent flow regime, AIChE J. 42 (1996) 2627–2634.

[33] R. Krishna, J.W.A. de Swart, J. Ellenberger, G.B. Martina, C. Maretto, Gas hold-up in slurry bubble columns, AIChE J. 43 (1997) 311–316.
[34] H.M. Letzel, J.C. Schouten, C.M. van den Bleek, R. Krishna, Influence of elevated pressure on the stability of bubbly flows, Chem. Eng. Sci. 52 (1997) 3733–3739.
[35] H.M. Letzel, J.C. Schouten, C.M. van den Bleek, R. Krishna, Influence of gas density on the large-bubble hold-up in bubble column reactors, AIChE J. 44 (1998) 2333–2336.
[36] R. Krishna, J.M. Van Baten, J. Ellenberger, Scale effects in fluidized multiphase reactors, Powder Technol. 100 (1998) 137–146.
[37] R. Krishna, J.M. van Baten, Simulating the motion of gas bubbles in a liquid, Nature 398 (1999) 208.
[38] R. Krishna, M.I. Urseanu, J.M. Van Baten, J. Ellenberger, Rise velocity of a swarm of large gas bubbles in liquids, Chem. Eng. Sci. 54 (1999) 171–183.
[39] M.I. Urseanu, Scaling up bubble column reactors, PhD dissertation in Chemical Engineering, University of Amsterdam, Amsterdam, 2000.
[40] H.M. Letzel, J.C. Schouten, C.M. van den Bleek, R. Krishna, Gas hold-up and mass transfer in bubble column reactors operated at elevated pressure, Chem. Eng. Sci. 54 (1999) 2237–2246.
[41] R. Krishna, M.I. Urseanu, J.M. Van Baten, J. Ellenberger, Influence of scale on the hydrodynamics of bubble columns operating in the churn–turbulent regime: experiments vs. eulerian simulations, Chem. Eng. Sci. 54 (1999) 4903–4911.
[42] G.P. Van der Laan, A.A.C.M. Beenackers, R. Krishna, Multicomponent reaction engineering model for Fe-catalysed Fischer–Tropsch synthesis in commercial scale bubble column slurry reactors, Chem. Eng. Sci. 54 (1999) 5013–5019.
[43] R. Krishna, J. Ellenberger, C. Maretto, Flow regime transition in bubble columns, Int. Comm. Heat Mass Transfer 26 (1999) 467–475.
[44] C. Maretto, R. Krishna, Modelling of a bubble column slurry reactor for Fischer–Tropsch synthesis, Catal. Today 52 (1999) 279–289.
[45] R.M. Davies, G.I. Taylor, The mechanics of large bubbles rising through extended liquids and through liquids in tubes, Proc. R. Soc. London, Ser. A 200 (1950) 375–390.
[46] R. Collins, The effect of a containing cylindrical boundary on the velocity of a large gas bubble in a liquid, J. Fluid Mech. 28 (1967) 97–112.
[47] I.G. Reilly, D.S. Scott, T.J.W. De Bruijn, D. MacIntyre, The role of gas phase momentum in determining gas hold-up and hydrodynamic flow regimes in bubble column operations, Can. J. Chem. Eng. 72 (1994) 3–12.
[48] P.M. Wilkinson, A.P. Spek, L.L. Van Dierendonck, Design parameters estimation for scale-up of high-pressure bubble columns, AIChE J. 38 (1992) 544–554.
[49] H.P. Riquarts, Strömungsprofile, Impulsaustausch und Durchmischung der flüssigen Phase in Bläsensaulen, Chem. Ing. Tech. 53 (1981) 60–61.
[50] K. Bernemann, Zur Fluiddynamik und zum Vermischungsverhalten der flüssigen Phase in Blasensäulen mit längsangeströmten Rohrbundeln. PhD Thesis, University Dortmund, 1989.
[51] W.D. Deckwer, R. Burckhart, G. Zoll, Mixing and mass transfer in tall bubble columns, Chem. Eng. Sci. 29 (1974) 2177–2188.
[52] G.D. Towell, G.H. Ackerman, Axial mixing of liquids and gas in large bubble reactor, in: Proceedings of 2nd International Symposium Chem. React. Eng, Amsterdam, The Netherlands, 1972, pp. B3.1–B3.13.
[53] R. Wendt, A. Steiff, P.M. Weinspach, Liquid phase dispersion in bubble columns, Ger. Chem. Eng. 7 (1984) 267–273.
[54] W.D. Deckwer, Y. Serpemen, M. Ralek, B. Schmidt, Modeling the Fischer–Tropsch synthesis in the slurry phase, Ind. Eng. Chem. Process Des. Dev. 21 (1982) 231–241.
[55] I.C. Yates, C.N. Satterfield, Intrinsic kinetics of the Fischer–Tropsch synthesis on a cobalt catalyst, Energy Fuels 5 (1991) 168–173.
[56] M.F.M. Post, A.C. van't Hoog, J.K. Minderhoud, S.T. Sie, Diffusion limitations in Fischer–Tropsch catalysts, AIChE J. 35 (1989) 1107–1114.
[57] P.L. Mills, J.R. Turner, P.A. Ramachandran, M.P. Dudukovic, The Fischer–Tropsch synthesis in slurry bubble column reactors: analysis of reactor performance using the axial dispersion model, in: K.D.P. Nigam, A. Schumpe (Eds.), Three-Phase Sparged Reactors, Gordon & Breach, 1996.